Vibration Analysis of LIBRA INPORTs

R.L. Engelstad and E.G. Lovell

February 1985

UWFDM-617

Presented at the Sixth Topical Meeting on the Technology of Fusion Energy, San Francisco, CA, 3-7 March 1985; Fusion Technology, 8, 1884-1889 (July 1985).

FUSION TECHNOLOGY INSTITUTE

UNIVERSITY OF WISCONSIN

MADISON WISCONSIN

Vibration Analysis of LIBRA INPORTs

R.L. Engelstad and E.G. Lovell

Fusion Technology Institute
University of Wisconsin
1500 Engineering Drive
Madison, WI 53706

http://fti.neep.wisc.edu

February 1985

UWFDM-617

Presented at the Sixth Topical Meeting on the Technology of Fusion Energy, San Francisco, CA, 3-7 March 1985; Fusion Technology, 8, 1884-1889 (July 1985).

VIBRATION ANALYSIS OF LIBRA INPORTS

R.L. Engelstad and E.G. Lovell
Fusion Technology Institute, University of Wisconsin
1500 Johnson Drive, Madison, Wisconsin 53706
(608) 262-0944

ABSTRACT

ICF conceptual designs have been proposed in which flexible tubes conveying liquid metal are subjected to repetitive impulsive pressures. Because the tubes are vertical, very long and carry liquid metal, gravity gradient effects are substantial. The complete equation of motion is presented. Results are obtained for the vibrational mode shapes and corresponding frequencies of the tubes. It is shown that the gravity gradients can produce strong asymmetries in the mode shapes and shifts in the numerical values of the natural frequencies. Results of an approximate perturbation analysis are also presented to support the exact solution.

INTRODUCTION

A major problem in ICF reactor designs is the protection of the first wall from x-rays, neutrons, target debris and mechanical shock resulting from target ignition. A concept proposed by the staff of the University of Wisconsin Fusion Technology Institute (FTI) uses an annular tube bank for the cylindrical cavity of the reaction chamber. The arrangement of the cavity tube bank is shown in Fig. 1 for the light ion beam reactor LIBRA, a conceptual design jointly developed by FTI and the Kernforschungszentrum Karlsruhe, FRG. Individual vertical tubes, identified as INPORT units, are braided from continuous silicon carbide fiber to produce a flexible porous component.[1] Liquid lithium-lead, used as a coolant and breeder, flows axially within the INPORT and also through the tube wall to develop a thin exterior film (approximately 1 mm thick) as shown in Fig. 2. This layer protects the INPORT by absorbing target debris and x-rays.

The first two rows of these tubes are subjected to repetitive mechanical shock loading during operation. To avoid resonance problems, it is important to have accurate values for the natural frequencies of the INPORTs. It is also important to accurately characterize the mode shapes since requirements for close packing may result in mechanical interference. These issues will be addressed in the work which follows.

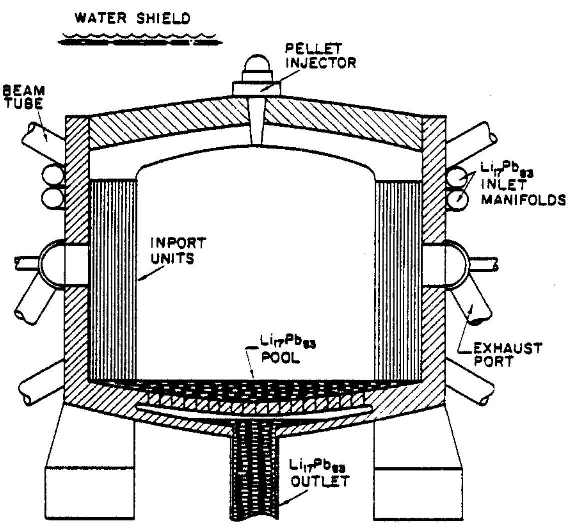

Fig. 1. Schematic of LIBRA Reaction Chamber.

INPORT MECHANICAL MODELING

The INPORTs are modeled as completely flexible tubes, neglecting any shear or bending resistance. They are elastically supported at the top and bottom as shown by the preliminary design of Fig. 3. This would permit relatively convenient assembly and allows tensile preloading of the INPORTs by means of the compression spring system. Thus the tubes react to the dynamic lateral loading with internal tension. In addition, a modification of this support mechanism can be used which allows end rotation, essentially as a ball-and-socket joint.

This dynamic analysis is developed for INPORTs comprising the first two rows of the annular tube bank since only these units receive the impulsive pressure from the blast wave.

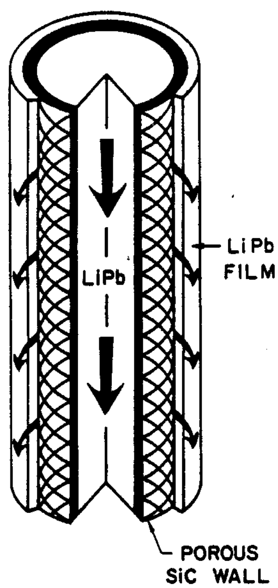

Fig. 2. Sectioned INPORT Unit.

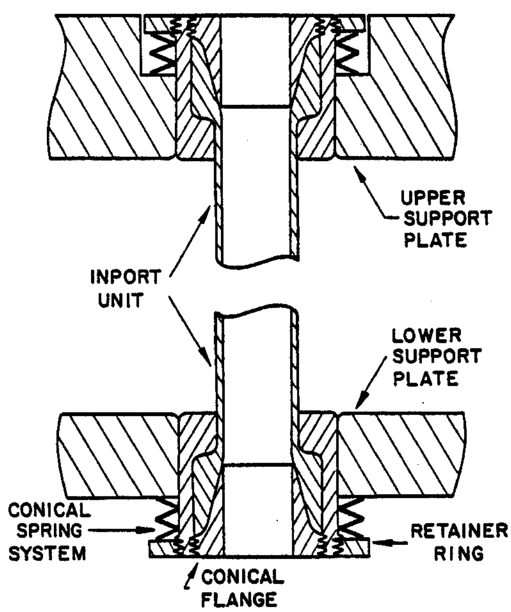

Fig. 3. Support Mechanisms for INPORTs.

These units have a diameter, thickness and length of 3 cm, 1 mm and 10 m, respectively. With the density of the lithium-lead being 9.44 g/cm^3, each tube has a mass of approximately 70 kg. Thus with a combination of an unsually large length and the heavy liquid metal, a substantial axial variation in internal tension will exist. In addition to these considerations it should be noted that the internal flow is retarded by a throttle mechanism at the lower end. The resulting pressure increase is included in the mechanical analysis.

GOVERNING EQUATION

The system under consideration (Fig. 4) consists of a uniform tube of length ℓ supported at each end. It has a cross-sectional area A_t, mass per unit length m_t and flexural rigidity EI. The internal fluid flows axially with velocity c, cross-sectional flow area A_f and mass per unit length m_f. The mean pressure within the tube is p, measured above atmospheric.

In its undeformed (equilibrium) position the longitudinal axis of the tube coincides with the x axis. With this vertical configuration, gravity effects will be assessed. Free and forced response of the tube is allowed in both the x-y and x-z planes along with longitudinal deformations.

With the compression spring mechanism (Fig. 3) supporting both ends, a static pretension T_o can be applied to the system. An additional axial tensile force is induced by the internal pressure, which is equal to $pA(1 - 2\nu)$ for a thin tube, where ν is Poisson's ratio. Nonlinear tension effects can be included by considering higher order terms in the expression for the tube extension. Also, since the weight of the viscid fluid is not negligible, there will be a tension variation due to a gravity gradient.

The general equations of motion for the tube were derived using Hamilton's principle and variational calculus procedures.[2] The resulting partial differential equation for lateral motion in the x-y plane is given by

$$
\begin{aligned}
&(m_t + m_f)\frac{\partial^2 v}{\partial t^2} + 2m_f c\frac{\partial^2 v}{\partial x \partial t} + m_f c^2 \frac{\partial^2 v}{\partial x^2} \qquad (1)\\
&+ \kappa_o(m_t + m_f)\frac{\partial v}{\partial t} - \frac{\partial}{\partial x}\Big\{T^*\frac{\partial v}{\partial x} + (EA_t - T^*)\\
&\Big[\frac{\partial u}{\partial x} - \Big(\frac{\partial u}{\partial x}\Big)^2 + \frac{1}{2}\Big(\frac{\partial v}{\partial x}\Big)^2 + \frac{1}{2}\Big(\frac{\partial w}{\partial x}\Big)^2\Big]\frac{\partial v}{\partial x}\Big\}\\
&+ EI\frac{\partial^4 v}{\partial x^4} - 3EI\Big(\frac{\partial v}{\partial x}\Big)^2\frac{\partial^4 v}{\partial x^4}\\
&- 12EI\Big(\frac{\partial v}{\partial x}\Big)\Big(\frac{\partial^2 v}{\partial x^2}\Big)\Big(\frac{\partial^3 v}{\partial x^3}\Big) - 3EI\Big(\frac{\partial^2 v}{\partial x^2}\Big)^3 = 0
\end{aligned}
$$

where

$$T^* = T_o - pA_f(1 - 2\nu) + (m_t + m_f)g(\ell - x)$$

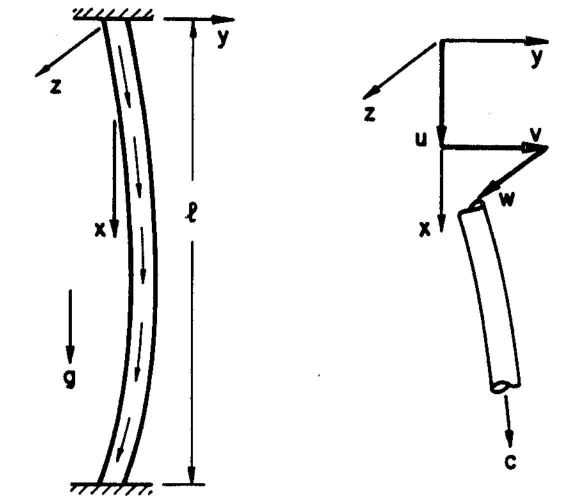

Fig. 4. Tube Geometry and Coordinate System.

and κ_o represents the coefficient of equivalent viscous damping.

PLANAR VIBRATIONS

In order to determine the basic modal characteristics of the tube, Eq. (1) has been linearized to decouple the lateral and longitudinal displacements. For transverse motion it is assumed that the effect of the Coriolis acceleration of the fluid, given by $2m_f c(\partial^2 v/\partial x \partial t)$, can be neglected. Also, since the INPORTs are considered as completely flexible tubes, Eq. (1) becomes

$$\frac{\partial}{\partial x}\{[(T_o - pA_f(1-2\nu) + (m_t + m_f)g(\ell - x) - m_f c^2]\frac{\partial v}{\partial x}\} - \kappa_o(m_t + m_f)\frac{\partial v}{\partial t} - (m_t + m_f)\frac{\partial^2 v}{\partial t^2} = 0 \ . \tag{2}$$

The equation of motion may be expressed in dimensionless terms by defining the following dimensionless quantities:

$$\bar{v} = \frac{v}{\ell}$$
$$\xi = \frac{T_o - pA_f(1-2\nu) + (m_t+m_f)g(\ell-x) - m_f c^2}{(m_t+m_f)g\ell}$$
$$\tau = \sqrt{\frac{g}{\ell}}\, t \tag{3}$$
$$\kappa = \sqrt{\frac{\ell}{g}}\, \kappa_o \ .$$

Substitution into Eq. (2) yields

$$\frac{\partial}{\partial \xi}\{\xi \frac{\partial \bar{v}}{\partial \xi}\} - \kappa \frac{\partial \bar{v}}{\partial \tau} - \frac{\partial^2 \bar{v}}{\partial \tau^2} = 0 \ . \tag{4}$$

Equation (4) can be reduced to an ordinary differential equation by assuming a harmonic solution of the form

$$\bar{v}(\xi,\tau) = \mathrm{Re}\{\phi(\xi)\bar{X}e^{i\bar{\omega}\tau}\} \tag{5}$$

where $\phi(\xi)$ is a complex function and $\bar{\omega}$ is the dimensionless frequency. Substitution of Eq. (5) into (4) gives

$$\frac{d}{d\xi}(\xi \frac{d\phi(\xi)}{d\xi}) + (\bar{\omega}^2 - i\kappa\bar{\omega})\,\phi(\xi) = 0 \ . \tag{6}$$

The solution to Eq. (6) involves Bessel functions of the first and second kind of zero order, namely

$$\phi(\xi) = AJ_o(\lambda\sqrt{\xi}) + BY_o(\lambda\sqrt{\xi}) \tag{7}$$

where

$$\lambda\sqrt{\xi} = \{4\bar{\omega}^2(\bar{T} - \frac{x}{\ell}) - 4i\kappa\bar{\omega}(\bar{T} - \frac{x}{\ell})\}^{1/2} \tag{8}$$

and the dimensionless tension and frequency are given by

$$\bar{T} = \frac{T_o - pA_f(1-2\nu) + (m_t+m_f)g\ell - m_f c^2}{(m_t+m_f)g\ell} \tag{9}$$

$$\bar{\omega} = \sqrt{\frac{\ell}{g}}\,\omega \ . \tag{10}$$

For a general solution A and B must be complex constants.

Finally, the complete solution to Eq. (4) can be expressed as a superposition of an infinite set of the normal modes of the tube, i.e.,

$$\bar{v}(\xi,\tau) = \mathrm{Re}\{\sum_{n=1}^{\infty} \phi_n(\xi)\bar{X}_n e^{i\bar{\omega}_n\tau}\} \tag{11}$$

which also includes the complex constant

$$\bar{X}_n = X_n e^{i\alpha_n} \tag{12}$$

where X_n and α_n are determined by initial conditions.

For convenience Eq. (11) has been rewritten so it contains only the real part

$$\bar{v}(\xi,\tau) = \sum_{n=1}^{\infty} X_n[A_{Rn}J_{oR}(\lambda_n\sqrt{\xi}) - A_{In}J_{oI}(\lambda_n\sqrt{\xi}) + B_{Rn}Y_{oR}(\lambda_n\sqrt{\xi}) - B_{In}Y_{oI}(\lambda_n\sqrt{\xi})] \cos(\bar{\omega}_n\tau - \alpha_n) - X_n[A_{Rn}J_{oI}(\lambda_n\sqrt{\xi}) + A_{In}J_{oR}(\lambda_n\sqrt{\xi}) + B_{Rn}Y_{oI}(\lambda_n\sqrt{\xi}) + B_{In}Y_{oR}(\lambda_n\sqrt{\xi})] \times \sin(\bar{\omega}_n\tau - \alpha_n) \quad (13)$$

where R and I represent the real and imaginary parts, respectively.

To determine natural frequencies and mode shapes, the eigenfunctions $\phi_n(\xi)$ are required to satisfy the boundary conditions of the problem. This results in the following set of equations

$$\begin{aligned}
&A_{Rn}J_{oR}(\lambda_n\sqrt{\xi_1}) - A_{In}J_{oI}(\lambda_n\sqrt{\xi_1}) + B_{Rn}Y_{oR}(\lambda_n\sqrt{\xi_1}) - B_{In}Y_{oI}(\lambda_n\sqrt{\xi_1}) = 0 \\
&A_{Rn}J_{oI}(\lambda_n\sqrt{\xi_1}) + A_{In}J_{oR}(\lambda_n\sqrt{\xi_1}) + B_{Rn}Y_{oI}(\lambda_n\sqrt{\xi_1}) + B_{In}Y_{oR}(\lambda_n\sqrt{\xi_1}) = 0 \\
&A_{Rn}J_{oR}(\lambda_n\sqrt{\xi_2}) - A_{In}J_{oI}(\lambda_n\sqrt{\xi_2}) + B_{Rn}Y_{oR}(\lambda_n\sqrt{\xi_2}) - B_{In}Y_{oI}(\lambda_n\sqrt{\xi_2}) = 0 \\
&A_{Rn}J_{oI}(\lambda_n\sqrt{\xi_2}) + A_{In}J_{oR}(\lambda_n\sqrt{\xi_2}) + B_{Rn}Y_{oI}(\lambda_n\sqrt{\xi_2}) + B_{In}Y_{oR}(\lambda_n\sqrt{\xi_2}) = 0
\end{aligned} \quad (14)$$

where ξ_1 and ξ_2 have been used to represent ξ evaluated at $x = 0$ and $x = \ell$, respectively. For a nontrivial solution to (14) the n determinants of the terms multiplying the A's and B's must equal zero, i.e.,

$$\begin{vmatrix}
J_{oR}(\lambda_n\sqrt{\xi_1}) & -J_{oI}(\lambda_n\sqrt{\xi_1}) & Y_{oR}(\lambda_n\sqrt{\xi_1}) & -Y_{oI}(\lambda_n\sqrt{\xi_1}) \\
J_{oI}(\lambda_n\sqrt{\xi_1}) & J_{oR}(\lambda_n\sqrt{\xi_1}) & Y_{oI}(\lambda_n\sqrt{\xi_1}) & Y_{oR}(\lambda_n\sqrt{\xi_1}) \\
J_{oR}(\lambda_n\sqrt{\xi_2}) & -J_{oI}(\lambda_n\sqrt{\xi_2}) & Y_{oR}(\lambda_n\sqrt{\xi_2}) & -Y_{oI}(\lambda_n\sqrt{\xi_2}) \\
J_{oI}(\lambda_n\sqrt{\xi_2}) & J_{oR}(\lambda_n\sqrt{\xi_2}) & Y_{oI}(\lambda_n\sqrt{\xi_2}) & Y_{oR}(\lambda_n\sqrt{\xi_2})
\end{vmatrix} = 0 \quad (15)$$

where $n = 1,2,3, \ldots, \infty$. The solution procedure then involves choosing a value of $\bar{\omega}$, calculating the argument given by Eq. (8) and corresponding Bessel function, and finally checking the value of the determinant. After $\bar{\omega}$ is found, the relative values of the complex constants A and B can be determined from (14). This procedure is repeated until the number of modes identified is sufficient to completely describe the tube motion.

NUMERICAL RESULTS

An analysis was performed to determine natural frequencies and mode shapes for the special case of zero damping. The first ten natural frequencies computed are shown in Fig. 5. Calculations were performed letting $\bar{T}$ approach 1 since $Y_0(0)$ is negatively infinite. Figure 6 shows the first, second and tenth mode shapes for dimensionless tensions of 1.1 and 3.0. For convenience, each has been individually normalized. Asymmetry is considerably noticeable with the lower tensions. Figure 7 shows the shifts of the maximum amplitude and zero crossing for modes 1 and 2 due to the nonlinear effects of the tension. Consequently, as $\bar{T}$ becomes much greater than the weight the natural frequencies and mode shapes will approach that of a classic string.

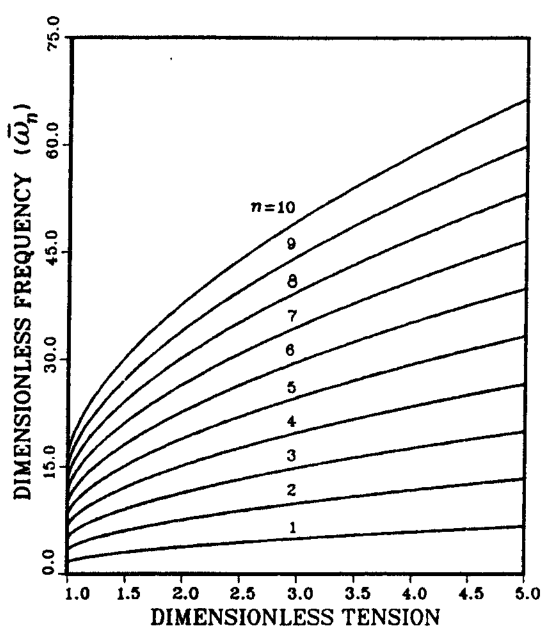

Fig. 5. Natural Frequencies of Heavy Tubes.

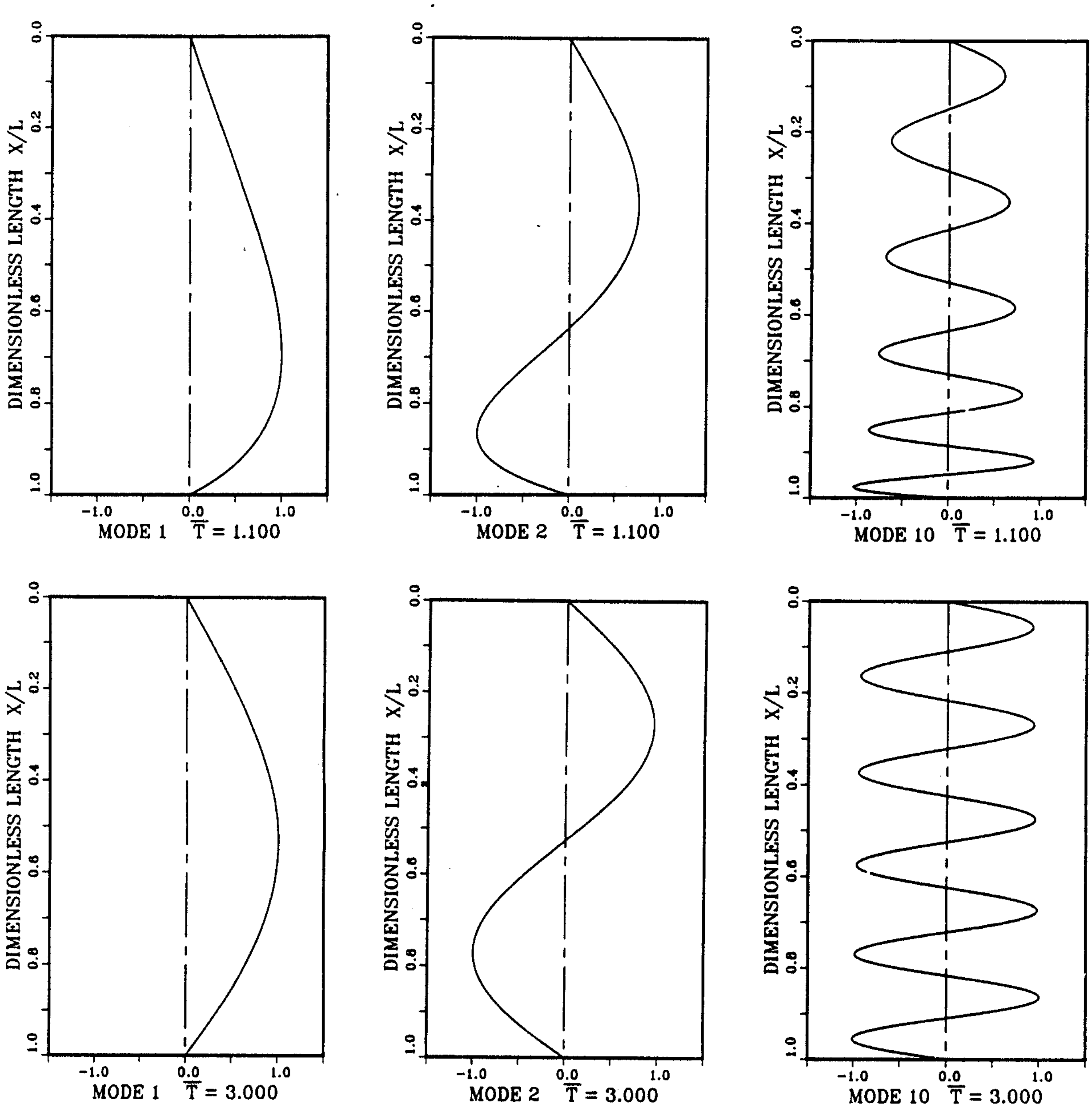

Fig. 6. The Fundamental, Second and Tenth Mode Shapes for Dimensionless Tensions of 1.1 and 3.0.

PERTURBATION ANALYSIS

The results from the exact solution can be verified to a limited degree by a perturbation analysis developed for the response of flexible tubes with small linear variations in the axial tension.[3]

The equations for natural frequencies and mode shapes are given by

$$\omega_n^2 = \left(T_e + \frac{W}{2}\right) n^2\pi^2/M\ell^2 \qquad (16)$$

$$\Phi_n(x) = \sin\frac{n\pi x}{\ell} - \frac{2W}{\pi^2 T_e}\sum_{m\neq n}\frac{mn}{(m^2 - n^2)}\left[\frac{1}{(n-m)^2} + \frac{1}{(n+m)^2}\right]\sin\frac{m\pi x}{\ell} \qquad (17)$$

where M and W represent the total mass and

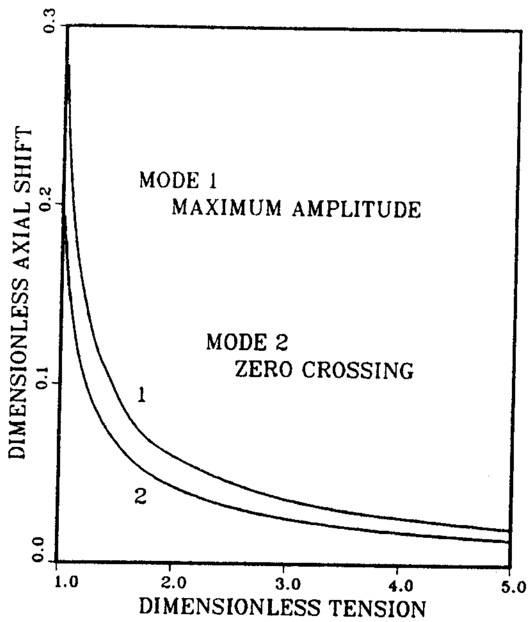

Fig. 7. Shifts in Locations of Maximum Amplitude and Zero Crossings.

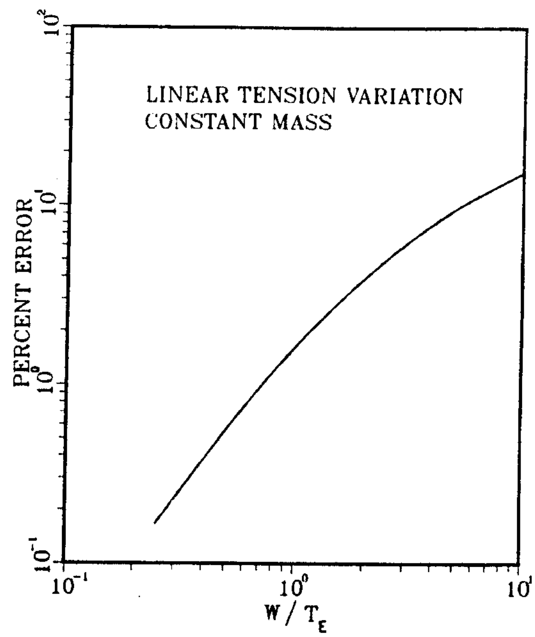

Fig. 8. Error in the Fundamental Frequency from the Perturbation Solution.

weight, respectively. The effective tension has been expressed as

$$T_e = (T_o - pA_f(1 - 2\nu) - m_f c^2) \ . \qquad (18)$$

For the mode shapes, the shifts in positions of maximum amplitude and crossing points are in good agreement. The differences between numerical values for frequencies from the two solutions are small, particularly for small tension variations. This is shown, for example, in Fig. 8 where a comparison is made for the fundamental frequency. The results for higher modes are similar. Thus, for cases characterized by significant tension variations, the exact solution is of greater importance.

CONCLUSIONS

Exact mode shapes and natural frequencies have been determined for completely flexible tubes in which an internal tension variation exists as a result of gravity in addition to axial preload. In comparison with the classic uniform tension problem, it has been shown that strong asymmetric changes can occur in the mode shapes, particularly for large gravity gradients. Similarly, the results show that the numerical values of the natural frequencies can also be substantially different for the same comparison. Both of these effects are important for the response calculations and design of INPORTs.

ACKNOWLEDGEMENT

This work was supported in part by Kernforschungszentrum Karlsruhe, Federal Republic of Germany, through Fusion Power Associates.

REFERENCES

1. G.L. KULCINSKI et al., "The INPORT Concept - An Improved Method to Protect ICF Reactor First Walls," Journal of Nuclear Materials, 103-104, 103-108 (1981).

2. R.L. ENGELSTAD and E.G. LOVELL, "Basic Theory for Three-Dimensional Motion of LIBRA INPORT Tubes," FPA-84-2, Fusion Power Associates (1984).

3. R.L. ENGELSTAD and E.G. LOVELL, "Planar Vibrations of LIBRA INPORT Tubes Including Gravity Gradient Effects," FPA-84-3, Fusion Power Associates (1984).